

Visible Spectrum Optical Communication and Distance Sensing for Underwater Applications

Felix Schill¹, Uwe R. Zimmer¹, Jochen Trumpf^{1,2}

¹Research School of Information Sciences and Engineering
The Australian National University, ACT 0200, Australia

and

²National ICT Australia Ltd., Locked Bag 8001, Canberra ACT 2601, Australia *

Felix.Schill@anu.edu.au

Abstract

To establish an underwater communication system for a swarm of submersibles, we developed an optical communication transceiver, small in size, combining the IrDA physical layer with 3 Watt high power light emitting diodes, emitting light in the green and blue part of the visible spectrum. This paper presents experimental results in air and under water. Furthermore, we show how this digital communication link can be used for accurate distance measurements without any modifications.

1 Introduction

Wireless underwater communication is a challenging task. Most commonly used methods, which are well established for digital communication in air, do not work in water. Available radio modules such as Bluetooth or Wireless LAN (802.11) operate in the gigahertz range, around 2.4 GHz. The attenuation in water for high frequency radio, especially in electrically more conductive salt water, is extremely high. Assuming an average conductivity of seawater of 4 mhos/metre, and 0.05mhos/metre in fresh water (tap water), the attenuation for 2.4GHz is around 1695dB/metre in seawater, and 189 dB/metre in freshwater. This is clearly not practical. A way around this is using ultra low frequency longwave radio, for which the attenuation is manageable, but the maximum bandwidth is significantly limited. We are currently developing a 8 kHz-122 kHz longwave radio system, with a maximum bandwidth

of 8192 bit/sec at 122 kHz. Sonar communication is another possibility, but available modems and transducers are too large for our application, and very expensive. In this publication, we investigate optical communication. Infrared communication according to the IrDA standard (Infrared Data Association, <http://www.irda.org>) is often used for short range communication, and offers reasonable bitrates, but also can't be used straight away under water, since water is not transparent for the infrared part of the spectrum. We present an approach, which uses the IrDA physical layer modulation, but replaces the infrared light emitting diodes (LEDs) with high power green or blue LEDs, and also the photodiode with a type which is sensitive in the visible part of the spectrum.

Using IrDA modulation has the advantage, that highly optimised integrated circuits are readily available at very low prices. With up to 115 kbit/sec, the data bandwidth is absolutely sufficient for most underwater robotics purposes. We decided to use 57600 bit/sec, to find a compromise between reliability and speed. Using the same components, it is easily possible to reconfigure and increase the bandwidth up to 312.5 kbit/sec, if required.

The presented optical communication system will be used in a swarm of small, autonomous submersibles. Only 40 centimetres long, the *Serafina* is a 5 DOF submersible, equipped with a PowerPC microcontroller, 3-axis accelerometers and gyroscopes, pressure sensor, sonar, compass and batteries to allow completely self-contained operation for up to 10 hours. Our current efforts are to establish a communication system for underwater, inter-swarm communication. The data communicated within the swarm will mainly be swarm control parameters, map data, and preprocessed sensor observations. While 57 kbit/sec might appear slow, it is sufficient for the relatively small data volumes that have

*National ICT Australia is funded through the Australian Government's *Backing Australia's Ability* initiative, in part through the Australian Research Council

to be exchanged. Since the swarm is expected to be much larger than the communication range of an individual submarine, the net bandwidth for the whole swarm scales up.

One communication subsystem will be the optical link presented in this paper, which offers high data rates up to 57 kbit/sec or more, in a range of 1-2 metres. This will be combined with a longwave radio transceiver, which offers only 8 kbit/sec speed, but a longer range of 10 metres. Major constraints are the limited available space on the craft, which asks for highly integrated circuits, low power consumption, and furthermore availability and price of the required components. We want to achieve a communication range of more than one metre, omnidirectional coverage (using several transceivers), small size (a few cubiccentimetres), and low cost (less than \$50 per transceiver).

There are some existing publications on optical underwater communication. Bales and Chryssostomidis presents a high speed transceiver, which achieves up to 10 Mbit/sec and has a long range of up to 20 metres. This is achieved by using highly specialised and expensive hardware, and powerful, directed light transmitters. A recent publication by [Tivey *et al.*, 2004] shows a compact, low-cost optical transceiver for underwater applications, with a range of 2.7m, also using the IrDA physical layer. Being 5cm in diameter and 10cm long, their device is yet still too large for our application, and has a speed of only 14.4 kbit/sec. Also, the narrow opening angle of their transmitter makes it difficult to achieve omnidirectional coverage, despite the 22 LEDs used in the transmitter. It must be noted that these transceivers were designed for much larger submersibles.

2 Choosing the best wavelength

Finding the optimal wavelength for underwater communication is a difficult task, and depends on many factors. It is well known that light absorption in water increases towards the red and infrared part of the spectrum. Minimal absorption is usually achieved for blue light around 400-450nm. This is only true for clear water, though - aquatic particles like chlorophyll, algae, or plankton have specific absorption patterns, which might lead to an absorption minimum at different wavelengths ([Babin and Stramski, 2002]). This is known as Rayleigh scattering. Finally, the availability of high power LEDs, their luminance, and also the sensitivity of the photodiode for different wavelengths play an important role. The best wavelength for the desired application depends strongly on the implementation and the environment, and can only be found experimentally. Results for the current implementation and clear water are presented later on.

3 Light sources

The recent development in LED technology offers great light intensity, fast switching speed, and small packages. Especially the availability of 3 Watt LEDs with superior luminous flux makes underwater optical communication possible. We chose the Luxeon III Emitter by Lumileds ([Lumileds, 2004]). It is available in many different colors, particularly in the wavelengths 460 nm (blue), 490 nm (cyan), and 520 nm (green). The typical opening angle is 50 degrees off axis (or 100 degrees total) at 80 % relative brightness (compared to the brightness on the optical axis), and 60 degrees at 50 % relative brightness. At the maximum average forward current of 1000 mA and forward voltage of 3.9 V, they offer 80 lumen of luminous flux for green and cyan, respectively 30 lumen for the blue emitter. This is approximately 20-50 times brighter than most other ultrabright LEDs. Combined with the wide opening angle, omnidirectional optical communication becomes feasible.

4 Transceiver implementation

For the experiments presented in this paper, a prototype transceiver was developed. It consists of two separate units - a sending unit, and a receiving unit. In the experiments, the sending unit and the receiving unit are separated, to test unidirectional communication. In the final implementation, every communication partner will be equipped with both a sender and a receiver. The major design criteria were a range which is at least one metre under water, and also low costs, small size and simplicity, since the optical transceiver will be used in swarms of small submersibles. The prototype transceiver as implemented costs approximately AUS\$ 45 per unit.

In order to simplify development and production, and also to profit from existing experience in proven technologies, the IrDA physical layer protocol was chosen and adapted to our needs. For greater flexibility in swarm applications, the higher levels of the IrDA protocol, which have been designed mainly for point to point connections, were discarded. Instead, our implementation only offers a stream-based serial optical broadcast link, which can be interfaced to a UART compatible interface. On this low hardware level, no link management or higher level error correction is done. Theoretically it is possible to operate in full duplex mode, but special care has to be taken to avoid reception of reflected light. Since the details of error correction, time multiplexing and network management are strongly application dependent, these options are left open, and are not dealt with in this paper.

The main changes to the IrDA physical layer specifications are the change of wavelength, optical characteristics such as opening angle and light intensity, and the

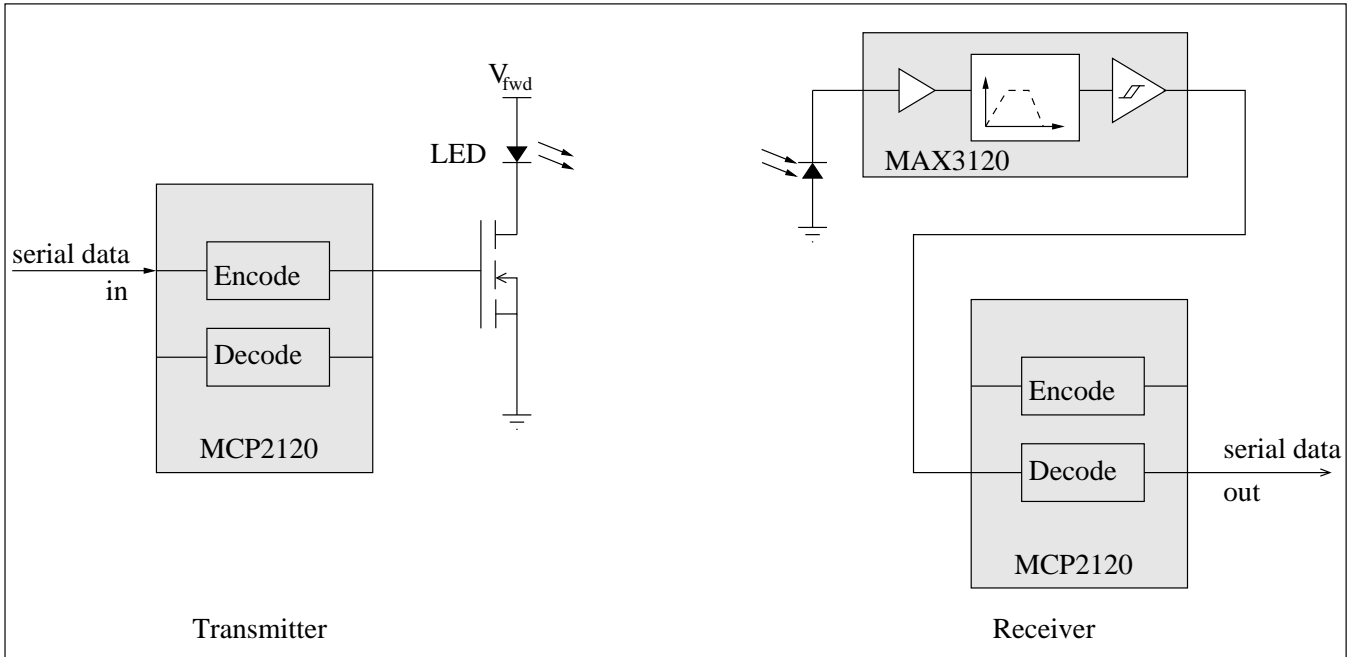


Figure 1: Block diagram of the transceiver

possibility of a full duplex mode. The implementation details are outlined in the following sections. Refer to figure 1 for a schematic diagram.

4.1 Transmitter

The transmitter accepts data over a UART compatible serial interface, encodes the data according to IrDA specifications, and generates light pulses in the visible spectrum, using high power LEDs. For encoding, a standard IrDA encoder/decoder chip is used (the MCP2120 by Microchip [Microchip, 2001]). The output of the infrared encoder controls the MOSFET power stage, driving the high power LED. As a light emitter, we use the Luxeon III emitter described earlier, in the wavelengths 460 nm (blue), 490 nm (cyan), and 520 nm (green). The power stage is designed in a way that it is possible to switch and choose between these three colours. To simplify the underwater experiments, the power stage/LED unit is separate from the encoder unit, and sits in a waterproof case.

The transparent domes of the LEDs are in direct contact with the surrounding water, to achieve optimal optical coupling. The emitters are unfocused, with the light emitting chip located in the focal point of the PMMA dome. This means that the light travels approximately perpendicularly through the boundary between dome and water, which minimises losses due to reflections. This also ensures a similar spatial emission footprint in air and in water.

The power consumption of the transmitter mainly depends on the forward voltage on the LED. For a nominal forward voltage of 3.9 V (80 lumen luminous flux), the average DC current during broadcast is 100mA (400mW power).

4.2 Receiver

The receiver circuit mainly follows IrDA guidelines, and uses standard components. To enable underwater operation, using visible light, a special photo diode has to be used, which is sensitive for wavelengths between 460 nm and 520 nm. We tested several different photo diodes, and got the best results with the diode SLD-70 BG2A, which has a good tradeoff between speed and sensitivity. The current from the photo diode is amplified by a high gain transimpedance amplifier, followed by a bandpass filter and a trigger, to retrieve the digital modulated signal. The amplification and filtering is implemented using the integrated circuit MAX3120 ([MAXIM-Semiconductors, 1998]). The filtered digital signal is then decoded by another IrDA encoder/decoder MCP2120. Even though one of these chips can already encode and decode IrDA signals, a separate chip is used for the receiver. The IrDA standard does not support full duplex data transmission, which means that the decoder is switched off while data is transmitted. This avoids that a sending device receives its own data, if light is reflected by nearby objects. For some applications outlined later on - especially the distance sensing

presented later - full duplex mode is necessary. By using two separate chips for transmitter and receiver, this problem does not occur. Also, this makes it possible to employ multiple independent receivers on one submersible, i.e. for different directions, and only one or also several transmitters.

The receiver is placed inside a small perspex box, the photo diode is aligned perpendicularly to the transparent floor of the box. There is room for improvement regarding the optical coupling to water, when mounting the receiver to the submersibles. For the experiments presented in this paper, this setup is sufficient.

5 Experiment setup

Experiments were carried out to measure the maximum range and coverage of the optical digital link in air and in water. The range is defined as the maximum distance between transmitter (LED) and receiver (photo diode), for which an error rate of 0% at full transfer rate can be maintained over at least several seconds. Furthermore, experiments were carried out to investigate how transfer rate and error rate behave at distances greater than the range of the link.

5.1 Measurement of error and transfer rate

Since the transceiver interface is a byte-oriented serial UART interface, the error rate measurement is also byte-oriented. The following approach was chosen to identify transmission errors:

The sender, connected to the transmitter, sends out a byte stream at full transfer rate of 57600 bits per second. Due to bit overhead, this corresponds to 6000 bytes per second. Bytes are sent out in ascending order, modulo 256. The receiver compares every received byte b_n with its predecessor b_{n-1} . If not $b_n \equiv b_{n-1} + 1 \pmod{256}$, then an error is counted. The error rate is measured over intervals of one second, as the errors over the number of received bytes. The criteria used in this paper is 0% error rate over an interval of one second, which means that 6000 consecutive bytes have been transmitted without any errors in one second. The transfer rate is measured as the number of received bytes per seconds.

There is a small possibility of false positives, when exactly 256 bytes were not received, and the next byte is correctly decoded. It is theoretically also possible that two consecutive bytes are both wrongly decoded in a way, that they exactly meet the requirement $b_n \equiv b_{n-1} + 1 \pmod{256}$. These cases are very unlikely, and do not play a role if the error rate is 0% at full transfer rate. It must be noted that this measurement does not give representative figures for the bit error rate, but it allows to identify error free transmission of data.

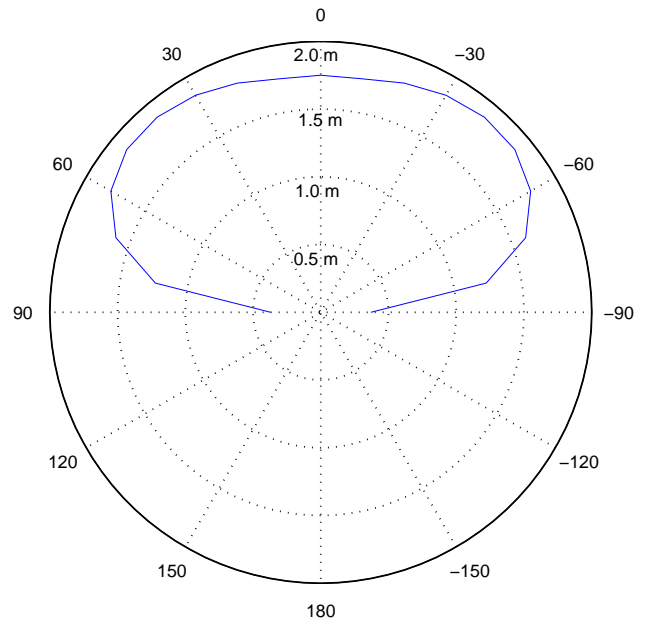


Figure 2: Angular coverage of the emitter (range for error-free transmission in air, cyan emitter, forward voltage 3.9V)

5.2 Hardware setup

In order to avoid any unwanted interferences and hidden transmission channels, sender and receiver were physically separated. For transmission, a microcontroller board was connected to the optical transmitter, which generated the described byte stream. The microcontroller board and the transmitter were powered by a laboratory power supply, operated from mains. The receiver circuit was battery powered, and connected to a laptop, which analysed the received bytes. The closest distance between sender and receiver unit was between the LED and the photo diode. The receiver unit was fixed. To measure the range, only the LED unit was moved.

For the experiments in air, the LED and the photo diode were aligned horizontally, and positioned well away from reflecting surfaces (> 0.5 m). The experiment was carried out in normal indoor lighting conditions, mainly fluorescent tubes.

The experiment in water was similar. The transmitter and receiver units were exactly identical. The experiment was carried out in a round pool with white walls, which is 1.5 metres deep, and 5 metres in diameter, in clear water with no visible pollution. To avoid effects of the reflecting water surface, the receiver was half-submerged, but floating on the surface, with the photo diode pointing downwards, approximately tilted 15 degrees away from the vertical pool wall, with 50 cm

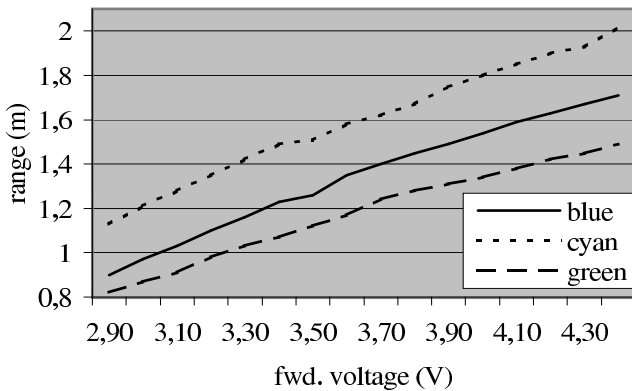


Figure 3: Range in air

clearance from the wall. The LED unit was submerged underneath the receiver, aligned with and facing the receiver. The experiments were carried out outside, at dusk, with slightly less environmental light than the experiments in air.

6 Results

Four experiments were carried out. The experiment setup and the individual results are outlined in the following section.

6.1 Range in air

The range in this context means the maximum distance between transmitter and receiver, which still allows error-free transmission of data. To measure the range, the distance between transmitter and receiver was increased to the point, where the error rate becomes larger than 0% over a time span of one second. The measurements were done for three different wavelengths, 460nm (blue), 490nm (cyan), and 520nm (green), and for different forward voltages in steps of 0.1 Volt. The forward voltage across the LED influences the luminous flux of the emitter. The results can be seen in figure 3.

As expected, the range increases approximately linearly (apart from an offset) with the forward voltage. This might be surprising at first, since the received light intensity decreases in squares with increasing distance. It must be considered, though, that with increasing forward voltage, the forward current through the emitter increases likewise. That means that the emitted power also goes up in squares, which explains the linear relationship. It is obvious that it can only be approximately linear within a range, since LEDs are nonlinear devices, and also heat effects can play a role at higher powers. The LEDs are only specified up to a forward voltage of 3.9 V, at a current of 1000 mA, for which the maximum luminous flux of 80 lumen is achieved (refer to the

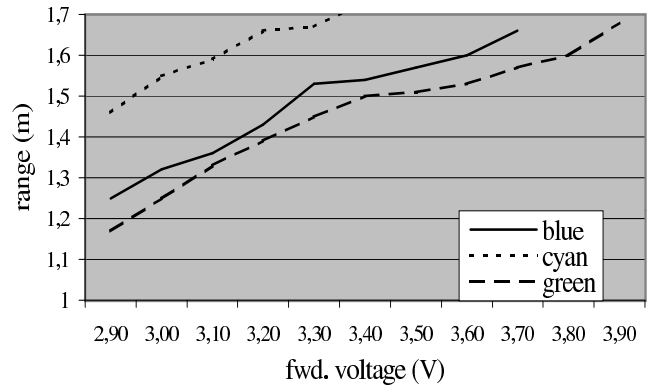


Figure 4: Range in water

datasheet for details). The maximum forward voltage in the experiments was 4.5 V, which is clearly over the manufacturer's specification. The emitters still worked stable and didn't overheat, since they were only driven by pulses with a short duty cycle, but a reduced lifetime might be the result.

As can be easily seen, the different wavelengths yield different ranges. Best range was achieved with the cyan emitter (2.02m), followed by blue (1.71m) and green (1.49m). The differences come from the wavelength dependent sensitivity of the photo diode, and also slightly different efficiencies of the emitters.

Figure 2 reveals that the range is almost uniform within a cone of 120 degrees opening angle (measured for 3.9 V forward voltage). The opening angle can easily be changed to meet the application by using lenses. The good uniformity allows for a communication link which is fairly direction independent.

6.2 Range in water

The same experiment as described before was conducted in water, in the pool setup described above. To our surprise, the range even increased, even though there should be absorption and coupling losses in water. Figure 4 shows the results. Unfortunately it was not possible to measure ranges greater than 1.7 metres, due to the limited depth of the pool.

The increased range can easily be explained by the small size of the pool environment. Light from the emitter is reflected by the bright pool walls, increasing the light intensity at the receiver. The LED is bright enough to visibly illuminate the whole pool. We also expect less high frequency noise disturbing the receiver in the outdoor pool environment, since there is no artificial light source such as fluorescent lamps. Also, water shields and reduces electrical interference at the highly sensitive receiver circuit.

The important result is that clear water attenuation in fresh water does not have a big impact on the range of optical communication up to a range of 1.7 metres, when using visible light in the blue and green range of the spectrum. Considering the huge impacts of water on HF radio, a range in the same order of magnitude is a good result. The relative difference in ranges of the three different wavelengths is still approximately the same. This also indicates that the attenuation in clear freshwater is low, so that the changing attenuation of different wavelengths does not have a big impact. While more precise measurements are not possible with our current equipment, the figures suggest an attenuation of less than 1 dB/metre. For our purposes, more precise results are not required.

6.3 Behaviour of the transfer rate for large distances

As a last experiment, the behaviour of the transfer rate for distances greater than the range was investigated. The results are shown in figure 5. For this experiment, the cyan emitter was used, with a forward voltage of 3.9 V. A range of 1.8 metres is expected. The region of interest for the behaviour of transfer rate and error rate is here above the range, from 1.8 metres to 2.7 metres. The transfer rate was measured and averaged over one second periods. The distance was increased continuously at a rate of one centimetre per second.

It can be seen how the transfer rate is very accurately linked to the distance. As the plot reveals, there is only a very small variation. It might appear counterintuitive at first, that a digitally decoded, synchronized bytestream shows such a predictable and almost linear decrease in the transfer rate over such a large range of distances, especially if considering that, at 2.7 metres, where the transfer rate almost becomes zero, the received light intensity is only 44% of the intensity at 1.8 metres.

This result suggests that the IrDA physical link layer approximates the additive white gaussian noise channel model (Binary Input AWGN). This means that noise is mainly generated on the receiver side, i.e. by the preamplifier and filter stage commonly used in IrDA applications. It is reasonable to assume that the optical transmission of light in air is almost noise-free. Also, the relatively short range doesn't allow for strong interference, scattering or reflection effects.

So why is the transfer rate decreasing? This is a side effect of the serial communication protocol. The start of a new byte is identified by a start bit. If the start bit couldn't be received, the IrDA decoder will reject the byte, which means a decrease of transfer rate. Therefore the transfer rate is an indirect measurement of the bit detection error.

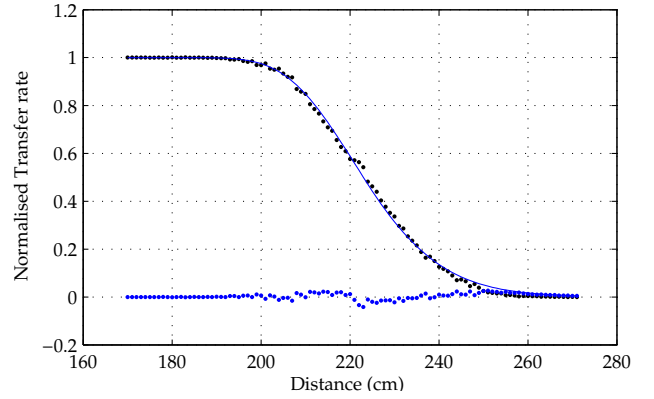


Figure 5: Transfer rate for increasing distance. Black dots represent the measured transfer rate, the blue curve is the fitted parameterised model, the blue dots are the error, i.e. the difference between model and data.

According to the AWGN channel model, the received analog signal is

$$Y(t) = X(t) + W(t) \quad (1)$$

where $X(t)$ is the transmitted signal, and $W(t)$ is white gaussian noise. This formula can be extended to include the transmission distance, assuming the transmitter is a uniform point source. To include ambient light into the model, the average light power P_{avg} received by the photo diode has to be included as well. The parameter α is for normalisation, and has to be identified experimentally.

$$Y(t) = \frac{\alpha}{d^2} X(t) + P_{avg} + W(t) \quad (2)$$

After preamplification, the signal goes through an adaptive comparator and trigger stage, which adapts to the average power level. The average power level can be measured by low-pass filtering. By comparing the incoming signal to this adaptive average, the digital pulse signal is recovered. This is a statistic process. The trigger accepts a pulse, if the received signal is greater than the average power level, plus a hysteresis term. So the decoded digital signal is

$$Y_d(t) = \begin{cases} 1 & \text{if } Y(t) > (P_{avg} + h) \\ 0 & \text{otherwise} \end{cases} \quad (3)$$

Therefore, the probability for receiving and decoding a pulse is

$$P(Y_d = 1|X) = P(Y - (P_{avg} + h) > 0) \quad (4)$$

$$= P\left(\frac{\alpha}{d^2} X + W - h > 0\right) \quad (5)$$

$$= P\left(-\frac{\alpha}{d^2} X + h < W\right) \quad (6)$$

$$= Q_\sigma\left(-\frac{\alpha}{d^2}X - h\right) \quad (7)$$

$$=: Q_\sigma(D(X)) \quad (8)$$

$$\text{with } Q_\sigma(u) := \int_u^\infty \frac{1}{\sigma\sqrt{2\pi}} e^{-z^2/(2\sigma^2)} dz$$

This probability is basically a function of the signal to noise ratio. The signal power is proportional to the inverse square of the distance, the noise level is specified by σ in Q_σ . The detection probability $Q_\sigma(D(X))$ can be rewritten to obtain parameters which are easier to calibrate. We can assume unit variance, and rescale the function $D(X)$:

$$Q_1(D'(X)) = Q_1\left(-\bar{\alpha}\left(\frac{1}{d^2} - \frac{1}{d_0^2}\right)X\right) \quad (9)$$

Here, the distance d_0 expresses the distance where the transfer rate is only 50%, and $\bar{\alpha}$ is a scaling factor, expressing the luminous flux of the LED and the sensitivity of the detector relative to the noise level. This function approximates the observed data astonishingly well. The fitted curve with $\bar{\alpha} = 400000$ and $d_0 = 223$ cm can be seen in figure 5. The absolute error is below 0.02, which is close to the measurement resolution.

7 Distance sensing

Though the main use of the optical communication system is data transfer between submersible swarm members, the observed behaviour of ranges and the transfer rate can also be used for distance sensing. This can be done without any changes to the hardware. This is useful to identify the swarm geometry, and to track communication partners. The following considerations assume that the receiver is within the uniform part of the angular coverage (within 60 degrees off axis). This restriction can be checked using a camera sensor, or can also be overcome by using several transmitters, to achieve overall uniform coverage. There are two general ways for measuring the distance between transmitter and receiver:

7.1 Short range distance measurements

If the receiver is within the 0% error rate range of the transmitter, the transfer rate and error rate don't reveal the signal strength, and therefore can't be used for distance measurements. In this case, it is possible to change the forward voltage at the transmitter, in order to identify the 0% error rate threshold.

Normally, the transmitter (or master) sends at the maximum nominal forward voltage (3.9V). When a receiver identifies and decodes the signal, this receiver can calculate transfer rate, and verify the 0% error condition.

If this is fulfilled, the receiver sends back a request for short range distance sensing. The master now slowly lowers the forward voltage, and while doing so, always sending out the currently measured forward voltage. This goes on as long as the receiver can decode the signal error-free. When the range boundary is reached for a specific forward voltage, this process can stop, and the receiver can calculate the range for the last correctly received forward voltage, using the range plot shown in figure 3 (This is a simple, linear function). This distance can be sent back at full power to the master, which then can abort the transmission.

It is of course also possible to implement this as a non-interactive process. In this case, every unit would send out a frame, where the forward voltage is swept down continuously, while again sending out the current voltage. Every receiver in range can then determine the error rate dropoff point individually, which is proportional to the distance. The short-range method has the advantage, that the identity of the receiver is known. This makes it easier to generate a geometric swarm model.

7.2 Long range distance measurements

If transmitter and receiver are so far apart, that an error-free transmission is not possible even at full power, it is still possible to measure the distance. Assuming the sender is transmitting an evenly distributed bit pattern at full speed, all the receiver has to do is to measure the current transfer rate, which stands in a close relationship with the distance (figure 5). Using a parameterised, calibrated function, or a lookup table, the distance can be retrieved.

Since error free communication is not possible over this long range, the identity of the sender is not known. This problem can easily be solved, if the optical communication system uses a time-sliced, collision-free sender arbitration protocol. In this case, the sending schedule is known throughout the network. Now it is easy to look up the current sender in the scheduling information, even if the transmission cannot be decoded correctly.

7.3 Limitations

Both approaches assume a homogenous environment, without any obstacles close to receiver, transmitter, or the line of sight. Reflections can disturb the measurements. Obviously, both curves for range and transfer rate over distance have to be experimentally measured for the given hardware setup, in order to calibrate the measurements. The calibration results can be stored as parameterised functions, or also as lookup tables. With proper calibration, the expected accuracy is better than 2 cm for both measurement methods.

The distance estimations can be affected by the water quality. For many swarm applications, this is not critical. Assuming homogenous visibility for the whole swarm, all distances are still relatively correct, up to a scaling factor. The scaling factor can be estimated using other sensors, or by combining dead-reckoning with distance measurements.

8 Conclusions

The presented optical communication system is suitable for underwater applications, uses cheap and easily available components, and can furthermore be used to reliably measure the distance between transmitter and receiver. It has been shown that the range is not decreased under water by clear water attenuation, for the wavelengths from 460 nm to 520 nm, and that recently available high power LED emitters can be successfully used for high speed optical communication. The wide angular coverage, the uniform emission footprint and very high light intensity allow for either omnidirectional coverage up to 2 metre radius with only five transmitters, or, with additional lenses, long range directional links using a collimated beam. The power consumption of 400mW per transmitter during transmission is manageable, even on small battery-powered submersibles. With the presented methods for distance measurement, the transmission power can easily be adjusted to the necessary range, in order to save power.

The reproducible, linear behaviour of the range allows accurate distance estimations by varying the forward voltage through the LED. For longer range distance measurements, the measured byte transfer rate can be used as an indirect measurement of the bit error rate. Experiments suggest that the optical link closely follows the AWGN channel model. The measured transfer rate allows an accurate estimation of the received signal strength, and therefore the distance between transmitter and receiver. This allows distance estimations with an accuracy better than two centimetres.

9 Future work

The prototype transceiver currently used for experiments will be redesigned, to achieve smaller physical dimensions, and to enable implementation on the submersible. Several transmitters and receivers will be used, to achieve omnidirectional, uniform coverage. The communication system will be combined with a camera sensor, which can easily track the visible, bright emitters of other submersibles, and pinpoint their precise angular location. The distance can be measured by the described optical communication system. The identity of the tracked transmitter is also known to the

communication system. This makes it possible to calculate the swarm geometry, to locate and position submersibles with respect to the swarm, or fixed active beacons in the environment. Once the swarm geometry is known, it is far easier to implement routing and broadcasting protocols, and to maintain links throughout the swarm.

The optical coupling of the emitters and photoreceptors to the water is an open field. Especially if wide opening angles and uniform emission footprints are required, coupling lenses have to be carefully designed, to avoid losses due to reflection, refraction, or occlusion.

Further experiments have to be carried out, to identify the effects of Rayleigh scattering and absorption in turbid water. On one hand, this will have an effect on the optimal wavelength for communication. On the other hand, it is unclear how scattering will affect the described decrease in transfer rate, and if the current model still holds. Also, the effect of obstacles and reflection of light by nearby objects has to be investigated. The next development step is the integration of transceivers into the submersibles, which will make it possible to carry out more experiments in open water, saltwater, at different depths and environments.

10 Acknowledgements

We would like to thank Alexander Bahr, Vinod Patmanathan and Ankur Agrawal for their contributions to the optical communication system.

References

- [Babin and Stramski, 2002] Marcel Babin and Dariusz Stramski. Light absorption by aquatic particles in the near-infrared spectral region. *Am. Soc. of Limnology and Oceanography*, 47(3):911–915, 2002.
- [Bales and Chryssostomidis, 1995] J. W. Bales and C. Chryssostomidis. High bandwidth, low-power, short-range optical communication underwater. In *Proc. 9th Int. Symp. on Unmanned Untethered Submersible Technology*, 1995.
- [Lumileds, 2004] Lumileds. Luxeon III Emitter, Technical Datasheet DS45, 2004.
- [MAXIM-Semiconductors, 1998] MAXIM-Semiconductors. MAX3120 Low-Profile, 3V, 120 μ A IrDA Infrared Transceiver, 1998.
- [Microchip, 2001] Microchip. MCP2120 infrared encoder/decoder, datasheet, 2001.
- [Tivey *et al.*, 2004] Maurice Tivey, Paul Fucile, and Enid Sichel. A Low Power, Low Cost, Underwater Optical Communication System. *Ridge 2000 Events*, 2(1):27–29, 2004.